BioMACROMOLECULES

Article

Self-Healing pH- and Enzyme Stimuli-Responsive Hydrogels for Targeted Delivery of Gemcitabine to Treat Pancreatic Cancer

Panayiotis Bilalis, Dimitrios Skoulas, Anastasios Karatzas, John Marakis, Athanasios Stamogiannos, Chrisida Tsimblouli, Evangelia Sereti, Efstratios Stratikos, Konstantinos Dimas, Dimitris Vlassopoulos, and Hermis Iatrou

Biomacromolecules, **Just Accepted Manuscript** • DOI: 10.1021/acs.biomac.8b00959 • Publication Date (Web): 10 Aug 2018

ACS Publications

is published by the American Chemical Society. 1155 Sixteenth Street N.W., Washington, DC 20036

Self-Healing pH- and Enzyme Stimuli-Responsive Hydrogels for Targeted Delivery of Gemcitabine to Treat Pancreatic Cancer

Panayiotis Bilalis,[1] Dimitrios Skoulas,[1] Anastasios Karatzas,[1] John Marakis,[2] Athanasios Stamogiannos,[3] Chrisida Tsimblouli,[4] Evangelia Sereti,[4] Efstratios Stratikos,[3] Konstantinos Dimas,[4] Dimitris Vlassopoulos[2] and Hermis Iatrou[1]*

1. University of Athens, Department of Chemistry, Panepistimiopolis, Zografou, 15771, Athens, Greece
2. FORTH, Institute for Electronic Structure and Laser, Heraklion 70013, Greece and University of Crete, Department of Materials Science & Technology, Heraklion 70013, Greece
3. National Centre for Scientific Research Demokritos, Patriarhou Gregoriou and Neapoleos 27, Agia Paraskevi 15341, Athens, Greece.
4. Department of Pharmacology, Faculty of Medicine, University of Thessaly, Larissa, Greece

Abstract. A novel, multifunctional hydrogel that exhibits a unique set of properties for the effective treatment of pancreatic cancer (PC) is presented. The material is comprised of a pentablock terpolypeptide of the type PLys-*b*-(PHIS-*co*-PBLG)-PLys-*b*-(PHIS-*co*-PBLG)-*b*-PLys which is a non-cytotoxic polypeptide. It can be implanted via the least invasive route and selectively delivers gemcitabine to efficiently treat PC. Simply mixing the novel terpolypeptide with an aqueous solution of gemcitabine within a syringe results in the facile formation of a hydrogel that has the ability to become liquid under the shear rate of the plunger. Upon injection in the vicinity of cancer tissue, it immediately reforms into a hydrogel due to the unique combination of its macromolecular architecture and secondary structure. Due to its pH responsiveness, the hydrogel only melts close to PC, thus the drug can be delivered directionally towards the cancerous rather than healthy tissues in a targeted, controlled and sustained manner. The efficacy of the hydrogel was tested *in-vivo* on human to mouse xenografts using the drug gemcitabine. It was found that the efficacy of the hydrogel loaded with only 40% of the drug delivered in one dose, was equally or slightly better to the peritumoral injection of 100% of the free drug delivered in two doses, the typical chemotherapy used in clinics so far. This results suggest that the hydrogel can direct the delivery of the encapsulated drug effectively in the tumor tissue. Enzymes lead to its biodegradation, avoiding removal by resection of the polypeptidic carrier after cargo delivery. The unique properties of the hydrogel formed can be predetermined through its molecular characteristics, rendering it a promising modular material for many biological applications.

Keywords: synthesis of polypeptides, self-healing hydrogels, targeted drug delivery, pH- and enzymatically stimuli-responsive, cancer

INTRODUCTION

While the overall incidence of cancer mortality has steadily decreased over the last several decades for most types of cancer, the mortality of pancreatic cancer (PC) is still increasing. PC is the fourth leading cause of all cancer-related deaths in the United States, fifth in Europe, and the seventh worldwide, while the 5-year survival rate is only 8%.[1] Compared to other cancers, PC has the unique property of high stromal-to-epithelial ratio which inhibits the formation and the function of blood vasculature, thereby diminishing drug delivery via perfusing blood, and thus through nanoparticles as nanocarriers.[2-4] Due to these barriers, the fraction of nanoparticles that penetrate the tumor cells may be less than 0.7%.[5] It is clear that with this tumor in particular, it is necessary to apply a local administration technology through drug-loaded implants rather than nanoparticulate drug carriers.

Drug-loaded implants are administered directly at the site of disease, offering the advantages of controlled and prolonged drug release, direct delivery to the site of disease, hence minimizing drug waste and reduced side effects due to the avoidance of systemic circulation of chemotherapeutic drugs. The best approach to achieve local drug release is through polymeric hydrogels because they can achieve effective, selective and sustained release in order to reduce patient morbidity.[6] Nearly all of the self-healing, pH- and temperature-responsive hydrogels considered so far are characterized by an ability to turn from viscous liquids in healthy tissue environment to hydrogels when injected within a cancer tissue. The sol-gel transition is due to shear thinning properties of the materials,[7-8] the higher temperature[9-15] and/or the lower pH[16-17] of the cancer tissue.[18-20] However, this mode of hydrogel formation can wound the cancer tissue, often leading to metastasis.

Clinical oncologists face two different situations: in the first, the PC tissue is developed in a localized place on the pancreas, which can be eliminated by resection. In this case a localized drug delivery system that will be placed on the resected tissue and selectively eliminate

remaining cancer cells that could cause relapse of the primary cancer or even initiate further metastasis is preferred. In the second situation, cancer is spread over the pancreas. Here, it is not possible to resect a part of the organ, and oncologists prefer a localized drug delivery system that would deliver drugs only to the pathological site but would remain inactive towards healthy tissue. In addition, the implant carrying the drug should be administered close to the cancer tissue with the most facile, controlled and less invasive way in order to reduce patient morbidity.

To meet these challenges, we envisaged a hydrogel that would operate in a completely different way when compared to most systems utilized so far. The non-cytotoxic hydrogel will exhibit shear-thinning properties, in order to be injected *in-situ* and transferred with the thinnest possible needle in order to be implanted in the least invasive way. The hydrogel should have the shortest possible self-healing time so as to be reconstructed quickly within the body and achieve a controlled deposition mechanism close to the cancer tissue. It should respond to the lower extracellular pH values of the cancer tissue, so as to melt in the vicinity of the pathological tissue, thus selectively delivering the drugs to PC tissue. The hydrogel would remain intact when in contact with the healthy tissue, minimizing the loss of the drug from this site. It should have buffering capacity in order to exhibit slow degradation rates and achieve slow and sustained drug release. In addition, it should be enzymatically biodegradable, so as not to require removal through resection after drug delivery (**Scheme 1**).

Recently, we have demonstrated the controlled polymerization of histidine. Poly(L-histidine) (PHIS) is the only pH-responsive amongst all homopolypeptides that undergoes a solubility transition within the physiological and tumor tissue pH and possesses many of the desired properties envisaged for the hydrogel.[21-27]

Herein, by using precise synthesis and living polymerization techniques, we present the synthesis of a series of novel amphiphilic pentablock terpolypeptides. After investigating their

properties, the nature of the amino acids as well as the molecular characteristics were carefully modified to develop a polypeptide that forms a multifunctional hydrogel exhibiting the optimum properties combined in one material in order to achieve effective drug delivery. As a proof of concept, we show that it is suitable to be used for the targeted local delivery of gemcitabine to PC without effecting healthy tissues, as confirmed by *in-vivo* studies in mice exhibiting human PC xenografts.

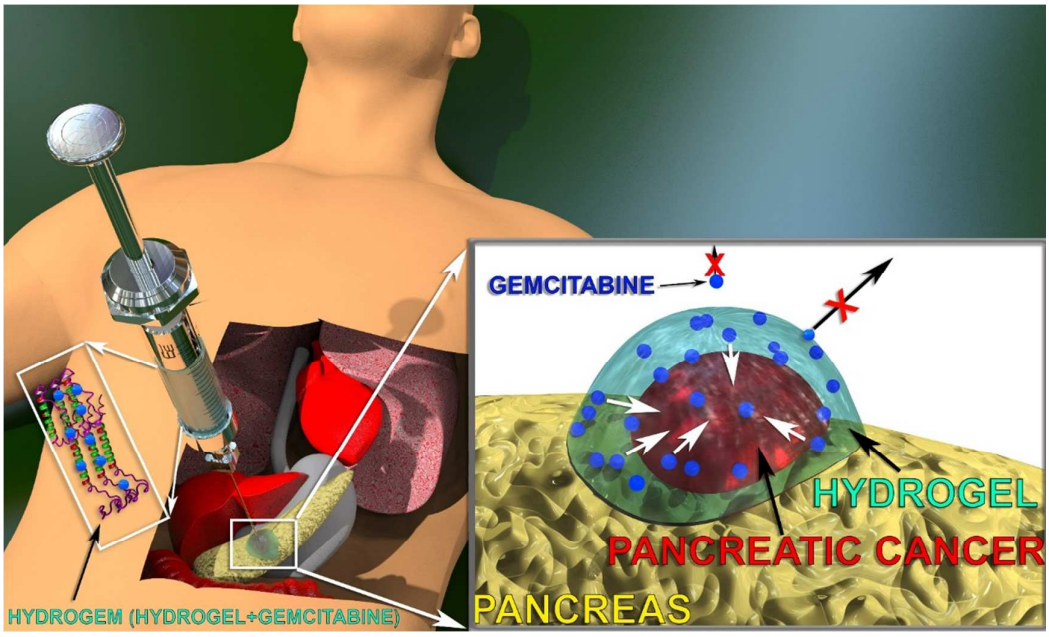

Scheme 1. Illustration of the chemical treatment of PC: the hydrogel with the encapsulated drug is implanted in the least invasive way and melts only in the vicinity of the cancerous tissue due to the lower pH, leading to a targeted and directional delivery.

EXPERIMENTAL SECTION

Materials and Methods

Materials. Boc-HIS(Trt)-OH (>99%) was purchased from SENNCHEM. Triphosgene (99%) was purchased from Acros Organics. Thionyl chloride (>99%), L-Lysine (>99 %), γ-Benzyl-L-glutamate and H-Leu-OH (>99 %) were purchased from Aldrich. Triethylamine (>99%,

Acros Organics) was dried over calcium hydride for one day and then distilled and stored in the vacuum line over sodium. The appropriate quantity needed was freshly distilled in a vacuum line. Purification of THF (dried, max 0.005% water, Merck) was performed using standard high vacuum techniques reported elsewhere.[1] Ethyl acetate (>99.5%, Merck) was fractionally distilled over phosphorous pentoxide. Hexane (>99%, Merck) was fractionally distilled over sodium. Dichloromethane was purchased by Merck. DMF (99.9+ %, special grade for peptide synthesis with less than 50 ppm of active impurities), the polymerization solvent, was purified by short-path fractional distillation under vacuum in a custom-made apparatus. The middle fraction was always used. Thiophene free benzene was treated with calcium hydride and it allowed to be stirred overnight to react with moisture. Then, it was distilled under high vacuum in a nearby flask containing n-BuLi, which reacted and stored.1,6-diaminohexane (98%, Alfa Aesar) was distilled fractionally under high vacuum and it was treated with sodium at room temperature for one day. Then, it was subsequently distilled into pre-calibrated ampules with break-seals. It was then diluted with DMF to the appropriate concentration in a sealed apparatus equipped with pre-calibrated ampules and kept away from light. Diethyl ether was purchased from Aldrich. Trifluoroacetic acid (TFA) (>99 %) was purchased by Merck. Fluorescamine and Trypsin were purchased from Aldrich.

Instrumentation. Size-exclusion chromatography. Size-exclusion chromatography (SEC) was used to determine the M_n and M_w/M_n values. The analysis was performed using a SEC equipment composed of a Waters 600 high pressure liquid chromatographic pump, Waters Ultrastyragel columns (HR-2, HR-4, HR-5E and HR-6E), a Waters 410 differential refractometer detector and a Precision PD 2020 light scattering detector at 60^{o}C featuring two detectors at 15^0 and 90^0 (TALLS). A DMF solution containing 0.1N LiBr was used as an eluent at a rate of 1mL/min, operating at 60 ^{o}C.

NMR spectroscopy. ^{1}H NMR spectroscopy (300 MHz) were performed using a Varian Unity Plus 300/54 spectrometer. The spectra of the NCAs were taken in $CDCl_3$ at room temperature.

FTIR. FTIR measurements were performed with a Perkin Elmer Spectrum One instrument, in KBr pellets at room temperature, in the range 450-4000 cm^{-1}.

Circular Dichroism. Circular Dichroism was performed with a Jasco J-815 model, featuring a Peltier model PTC-423S/15 thermo stabilizing system. The cell used was 1 mm Quartz Suprasil. The aqueous solution of the PBLG/PHIS polymer with ratio of the monomeric units 50/50 had a concentration of $3.3x10^{-4}$ g/mL, while the aqueous solution of the PBLG/PHIS polymer with ratio of the monomeric units 70/30 at every pH had a concentration of $2.5x10^{-4}$ g/mL. The adjustment of pH was performed through addition of diluted HCl or NaOH.

Scanning electron microscopy. Scanning electron microscopy/SEM–EDS of the hydrogels was performed with a Jeol JSM-5600 equipped with Oxford EDS. Carbon grids were used. The preparation of the samples was performed first by quick deep freezing of a small amount of the hydrogels with liquid nitrogen, followed by freeze-drying to remove the water. Sputter coating of the samples with gold occurred prior the measurements.

Enzymatic Degradation-Fluorescence measurements. All fluorescence measurements were performed using a TECAN SPARK 10M multimode microplate reader using 96-well black microplates (Greiner). To measure the enzymatic degradation of the hydrogel by either Trypsin or Leucine Aminopeptidase (LAP), 2mg of hydrogel was mixed with 0,1nM Trypsin or 100nM LAP in PBS and incubated at 37 ^{o}C for 1 hour or 24 hours respectively. At the end of the incubation, a sample of 10 μL from the reaction was mixed with 90 μL of a solution of fluorescamine containing 1 mg/ml fluorescamine in acetonitrile, 15 μL of 0.1M borate buffer at pH 8.0 and 145 μL of MilliQ water. After 5 min, the fluorescence was measured using excitation at 405 nm and emission at 485 nm.

Synthesis of the Terpolypeptides.

A. Synthesis of the Monomers. The synthesis of the monomers, i.e. *ε-tert*-butyloxycarbonyl-L-lysine N-carboxy anhydride, N^{im}–trityl-L-histidine N-carboxy anhydride, *γ*-benzyl-L-glutamate N-carboxy anhydride as well as L-leucine N-carboxy anhydride has been presented in our previous publication,[21] and are given briefly in the SI.

B. Synthetic Approach of the Polypeptides.

The polypeptides were synthesized using high vacuum techniques.[28-29] The polymerization reactors were designed to have volumes at least three times larger than that of the CO_2 generated by each polymerization. Polymerizations were carried out with 1,6-diaminohexane as the initiator. Briefly, in a solution of *ε-tert*-butyloxycarbonyl-L-lysine N-carboxy anhydride in DMF (Lys-NCA), an *α,ω*-hexamethylenediamine solution in DMF was added. After completion of polymerization (middle block), appropriate amounts of N^{im}-trityl protected L-histidine N-carboxy anhydride (HIS-NCA) and *γ*-benzyl-L-glutamate N-carboxy anhydride (BLG-NCA) (molar ratio 1:1) were dissolved in DMF and added to the reaction flask. The polymerization was allowed to continue for 6 days (two hydrophobic blocks). Lys-NCA was then added, followed by precipitation in diethylether after the completion of the polymerization. The selective cleavage of *trityl* and *tert*-butyloxycarbonyl groups from poly(L-histidine) and poly(L-lysine) segments, respectively, was achieved by treating with trifluoroacetic acid (TFA), followed by addition of triethyl silane. The solution was precipitated in diethylether, and the white solid was filtered and dried. The deprotected pentablock was then mixed with MilliQ water and dialyzed (membrane molecular weight cut off 3500 Daltons) against dilute HCl solution (pH = 3) for 2 days, dilute NaOH solution (pH = 8) for 2 days and DI water for 2 days (for each step the water changed every 12 h). Finally, the solution was lyophilized in order to obtain the final pentablock terpolypeptide as a white

powder. A similar procedure was followed for the synthesis of the terpolypeptides exhibiting poly(L-leucine) (PLEU) instead of PBLG.

Formation of Empty Hydrogels and Hydrogels Loaded with Gemcitabine.

Pentablock terpolypeptide hydrogels were prepared very simply by adding MilliQ water in a vial containing the solid polypeptide. After 2-3 hours, the hydrogel was ready without requiring any other treatment. The water swelled the polypeptide, keeping the general shape of the initial solid. Pentablock terpolypeptide hydrogels loaded with gemcitabine (Hydrogem) were prepared by first dissolving the appropriate amount of gemcitabine in pyrogen-free MilliQ water (gemcitabine:polypeptide ratio 1:1 (w/w)), at 35 ^{o}C, followed by addition of the warm gemcitabine solution to the polypeptide. The temperature was kept at 35 ^{o}C until complete swelling of the polypeptide and formation of homogeneous hydrogel, about 3-4 hours. In order to ensure the formation of a homogeneous mixture, the hydrogel was inserted into a syringe and passed between two syringes multiple times using a syringe connector, prior to the *in-vivo* tests. The hydrogel was stable at room temperature for several days, while the same gemcitabine solution in MilliQ water precipitated after 0.5 hours when the temperature was lowered to 20 ^{o}C.

Culture of Pancreatic Cancer Cells

AsPC-1 human PC cell line (adenocarcinoma derived from ascites) purchased by ATCC (ATCC-LGC, Germany), was cultured in RPMI 1640 medium (Gibco, Grand Island, NY, USA) supplemented with 100U/ml penicillin + 100µg/ml streptomycin (Gibco, Grand Island, NY, USA), 2mM L-glutamine (Gibco, Grand Island, NY, USA), 5% fetal bovine serum (Lonza, Verviers, Belgium), at 37°C in a humidified atmosphere containing 5% CO_2.

***In Vivo* Studies.**

For the *in-vivo* studies, NOD.CB17-Prkdc^{scid}/J mice purchased from Jackson Laboratory (The Jackson Laboratory 600Main Street Bar Harbor, Maine 04609 USA) were used. All animals for *in vivo* experiments were kept under specific pathogen free (SPF) conditions in type IIL cages, at the experimental unit of our department (Department of Pharmacology, EL42-BIO_Exp03, protocol license 5542/22806-30/11/2015) in a climate-regulated environment (21 ± 1°C; 50-55% relative humidity) under a 12 h/12 h (lights on at 7:00 AM) light/dark cycle and allowed *ad libitum* food and water. Female and male mice, 6–8 weeks old, were used in the studies described here. Handling and experimentation of animals complied with Greek laws (PD 56/2013 and Circular 2215/117550/2013) and the guidelines of the European Union (2013/63/EU).

Acute Toxicity Testing of the Empty Hydrogel. Acute Toxicity Testing was performed following the guidelines of the NCI (NCI, NIH, USA) protocol[30] for acute toxicity dosing. A single female mouse was given a single injection of 400 mg/kg, a second mouse received a dose of 200 mg/kg and a third mouse received a single dose of 100 mg/kg. The mice were observed for a period of 2 weeks. They were sacrificed if they lost more than 20% of their body weight or if there were other signs of significant toxicity.

In a preliminary experiment to select the least toxic form of hydrogel between PLEU and PBLG, three female mice received a single dose of hydrogel subcutaneous (sc) at the dorsal area of gemcitabine at 400, 200 and 100mg/kg (320, 160 and 80μl, respectively) of a 1/30 (w/w) hydrogel formulation and one received hydrogel intra-peritoneally (ip, 200mg/kg). Mice were observed daily for a total period of 2 weeks. For the needs of the experiments, the parameters probed and recorded were survival, weight loss and behavioral changes.

Gemcitabine Toxicity Testing. In the first experiment, gemcitabine (Gemsar VL7501, Farmaserve-Lilly) was administered to three male mice at three different doses (one dose/mouse). Gemcitabine (400, 200 and 100mg/kg) was administered in a single dose either ip or sc, and the mice were observed daily to detect and record any signs of toxicity.

Sub-chronic Toxicity of Gemcitabine. Gemcitabine was further evaluated for toxicity according to the administration schedule adopted for the efficacy studies. For this purpose, three mice received two injections of gemcitabine, ip or sc, at a week interval. Again, three gemcitabine doses were tested, 200mg/kg, 100mg/kg and 50mg/kg (one mouse per dose).

***In-Vivo* Efficacy Testing.**

To generate xenografts, exponentially growing cultures of AsPC-1 human PC cells were subcutaneously injected at the axillary region of the rear flank of 8 week-old male NOD.CB17Prkdc^{scid}/J mice from our animal facility ($1x10^6$ cells/injection, one injection/mouse). When the tumors reached a size of about 200mm^3 (advanced stage model) the mice were arbitrarily divided into 5 groups, each group consisting of 7 mice (7 tumors/group). Mice received A) empty hydrogel sc in the vicinity of the tumor (peritumoral administrations, pt) B) 100mg/kg gemcitabine ip C) 100mg/kg gemcitabine pt and D) 100mg/kg of gemcitabine loaded in hydrogel pt. All mice received two injections, once a week except for the group D mice that received only one injection at the beginning of the administration schedule. Another group of 7 mice received no treatment and served as the control group. In order to study the *in-vivo* effect of the compounds, mean tumor volume and standard deviation (SD) for all groups were calculated and growth curves were plotted as a function of time. Tumor volume was calculated according to the formula [(axb^2)/2], where a=length and b=width of the tumor as measured with a vernier's caliper (measurements were performed twice a week). Activity of the compounds was further evaluated by calculating the

tumor growth inhibition (% DT/DC ratio).[31] The DT/DC ratio represents the mean tumor volume for the treated groups versus control. DT and DC were calculated as the (mean tumor volume at day X) - (mean tumor volume at the first day of the treatment), in treated and control groups respectively. Mice remained in the study until the tumor volume reached a size of approximately 1600-1800mm^3 and were then euthanized. Mice were also weighed to monitor toxicity twice a week.

Rheology.

The polypeptides were characterized by means of dynamic oscillatory measurements using a sensitive strain-controlled rheometer (ARES 100FRTN1 from TA, USA). They included a) Dynamic frequency sweeps with a strain $\gamma = \gamma_0 \sin \omega t$ in order to probe the viscoelastic relaxation spectrum, i.e., the frequency dependent storage (G') and loss (G'') moduli in the range 0.01 – 100 rad/s. The stress response was $\sigma = \sigma_0 \sin(\omega t + \delta) = \gamma_0(G' \sin \omega t + G'' \cos \omega t)$ with σ_0 being the stress amplitude and δ the phase angle ($\delta = G''/G'$); b) Dynamic strain sweeps at constant frequency ω (typically 1 rad/s) and continuously increasing strain amplitude γ_0 from 10^{-3} to 3 strain units, in order to determine the limits of linear viscoelasticity and at the same time to explore the nonlinear response; c) Dynamic time sweeps at low frequency (typically 1rad/s) and a linear strain amplitude, with duration long enough to ensure that steady state was reached. In order to ensure that the measurements were reproducible, they were proceeded by a time sweep at large strain amplitude in the nonlinear regime (typically at strain amplitude of 2 strain units) or steady shear measurements at different rates (from $1s^{-1}$ to $100s^{-1}$) in order to shear-melt the structure (rejuvenation process), and a subsequent linear time sweep in order to reach steady state (the kinetic process toward steady state is the physical aging of the sample and, depending of its nature, it may relate to self-healing). This protocol allowed to erase the sample's mechanical history

(possible residual stresses during sample preparation and loading) and ensuring reproducible initial conditions for the measurements. The measurements were performed with a stainless steel cone-and-plate geometry (diameter 25 mm, cone angle 0.1 rad) and the temperature was controlled by means of a Peltier element. To minimize the risk of solvent evaporation, two approaches were implemented depending on sample availability. One consisted of effectively sealing the measred specimen with a non-volatile immiscible low-viscosity fluid (silicon oil of viscosity 5 mPas) by means of a home-made cyclindrical collar that was placed around the cone. The other made use of a home-made solvent trap that saturated the atmosphere around the specimen with solvent.

Statistical Analysis.

Statistical analysis was performed using ANOVA or student's t-test and the GraphPad Prism ver. 6 software package (GraphPad Software, Inc. La Jolla, USA). A $p<0.05$ was considered as statistically significant.

RESULTS AND DISCUSSION

A. Synthesis and Characterization of the Polypeptides.

The structure of the synthesized polypeptides is depicted in **Scheme 2**.

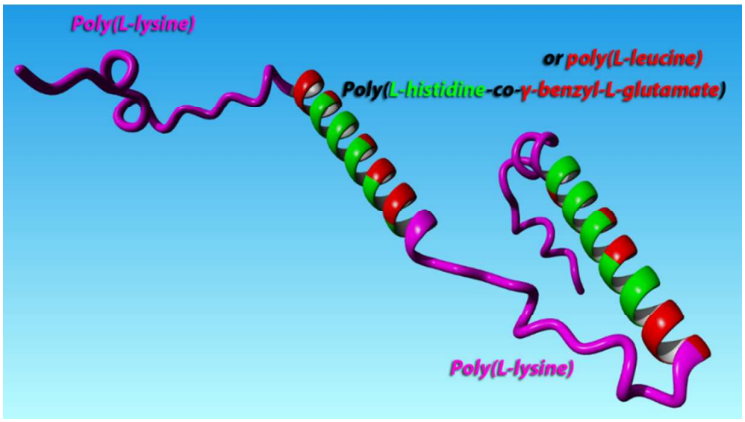

Scheme 2. Schematic illustration of the pentablock of the type PLys-b-(PHIS-co-PBLG (or PLEU))-b-PLys-b-(PHIS-co-PBLG (or PLEU))-b-PLys.

The synthetic strategy for the preparation of the terpolypeptides containing PBLG is shown in **SI Figure S12**. A similar strategy was followed for the synthesis of the terpolypeptides containing L-Leucine. These terpolypeptides are composed of one middle hydrophilic block (PLys), two hydrophobic blocks poly(L-histidine-*co*-*γ*-benzyl-L-glutamate (or L-leucine)), followed by two hydrophilic blocks of PLys, each one connected at the outer sides of the hydrophobic blocks. The middle hydrophilic block of poly(L-lysine) should have a high molecular weight in order to form strong hydrogels at very low concentrations, i.e. 3.33 % (w/w) in water.[32] In order to determine the influence of the PBLG composition on the properties of the hydrogel, we synthesized a series of pentablock terpolypeptides, with the poly(L-lysine) blocks (middle and outer) always being the same. The middle block had approximately 200 monomeric units, while the outer blocks had 60 monomeric units each, close to 120 monomeric units in total. We found that these PLys block dimensions were optimal for the development of the desired combination of properties of the pentablocks, mainly concerning the hydrogel strength, and will be presented in a forthcoming paper. In order to fine-tune and incorporate the desired stimuli-responsive properties on the hydrogel, the PHIS/ PBLG (or PLEU) monomeric ratio in the hydrophobic blocks was varied as 100/0, 70/30, 50/50 and 30/70. Since the PLys blocks were almost equal for all the polypeptides, the code of the pentablocks was defined by the PHIS/PBLG ratio, therefore the abbreviation PHIS70 refers to the pentablock with 70% monomeric PHIS units.

The synthesis was performed using high vacuum techniques.[28] The purity of the NCA monomers is crucial for their successful living polymerization utilizing ROP through primary amine difunctional initiator,[29] and was confirmed by FT-IR and NMR spectroscopy analysis, already discussed in our previous publication.[21] The random distribution of the copolymerized BLG and HIS-NCAs was proved through the solubility of the triblock copolypeptide resulting from their copolymerization. In case the polypeptides were block rather than random

copolymers, the PHIS block would be insoluble in DMF, while all our polymerizations where homogeneous, proving the random distribution of the two monomers. The selective deprotection of histidine and lysine monomeric units, while the benzyl groups of glutamic acid remain intact, is very important for the functionality of the polypeptide through the control of their secondary structure. It is well known that *Boc*- and *Trityl*- groups can be orthogonally cleaved under acidic conditions in the presence of the benzyl protected group of glutamic acid.[33-34] In addition, the dialysis procedure plays an important role in the pH neutralization and purification of the final polypeptide. It was very crucial to add a precise amount of base to the solution of the terpolypeptide during the dialysis procedure up to the value pH=8. This was tested by neutralization either at pH=7.0 or 9. When the neutralization was achieved at a lower value of pH=7.0, PHIS was partially neutralized, and addition of an aqueous solution of gemcitabine in water resulted in a liquid instead of the hydrogel. On the other hand, when the solution was brought to pH≥9.0, the polypeptide did not swell to form a hydrogel, and remained solid eventually precipitating. This was due to the neutralization, not only of PHIS but partially also of poly(L-lysine), rendering neutralized PLys hydrophobic, hence resulting in the lower solubility of the polypeptide and preventing hydrogel formation. A detailed description of the synthetic approach and purification of the polypeptides is given in the **SI pages 13-19**. The completion of the polymerization and deprotection processes was monitored by FTIR spectroscopy (**SI Fig. S13**). The final lyophilized polypeptides were excessively characterized by Size Exclusion Chromatography featuring two angle laser light scattering detector (SEC-TALLS) and FT-IR spectroscopy (**SI Fig. S13, S14**).

We initially synthesized the pentablocks containing poly(L-histidine-*co*-L-leucine) (PHIS-*co*-PLEU) with PLEU/PHIS monomeric unit % ratios of 0/100 10/90, 30/70, 50/50 and 70/30. Whereas most of these pentablocks formed strong hydrogels (e.g. 50/50 and 70/30) and responded to pH, the *in-vivo* acute toxicity tests showed that the hydrogels did not exhibit the

required cytotoxicity and durability in the body (**SI Fig. S27**). Therefore, we replaced L-leucine with γ-benzyl-L-glutamate (BLG), and the new hydrogel did not exhibit cytotoxicity in the acute toxicity tests for concentrations up to 400 mg/Kg, as required by the National Cancer Institute of USA (NCI) for materials to be used as drug carriers for cancer treatment. More importantly, by replacing LEU with BLG, the hydrogel properties were either maintained or improved. Details concerning the synthesis, molecular characterization, rheological properties of these polypeptides as well as the *in-vivo* tests are presented in the **SI Table 1**, **SI Figures S19, S20**.

The SEC-TALLS analysis of all terpolypeptides revealed a high degree of molecular and compositional homogeneity. The molecular characteristics of the pentablocks containing PLEU are given in **SI Table S1**. The SEC eluograms from the synthesis of pentablock terpolypeptide PLys-*b*-(PHIS-*co*-PBLG)-*b*-PLys-*b*-(PHIS-*co*-PBLG)-*b*-PLys HIS50 prior deprotection are depicted in **SI Figure S14**. The molecular characteristics of the polypeptides containing PBLG are listed in **Table 1**.

B. Ability of the Pentablocks to Form Hydrogels.

The ability of these polypeptides to form hydrogels by adding MilliQ water depended on two parameters: their molecular and compositional homogeneity and the PHIS/PBLG ratio. It was found that the pentablocks should be well-defined with a high degree of molecular and compositional homogeneity. If the polydispersity was high by intentionally mixing two different polypeptides, or by intentionally omitting one block, they either formed very weak hydrogels at higher polypeptide concentrations or did not gel at all. Regarding the PHIS/PBLG ratio, PHIS100 formed a weak hydrogel at room temperature (about 20 ^{o}C), while its strength was highly temperature-dependent, and at 37 ^{o}C it was transformed into liquid very quickly. PHIS70 did not form hydrogel at all, while PHIS50 and PHIS30 formed strong hydrogels, depending on the polypeptide concentration and the pH of water. When the

pH of the latter had a value of 6.6, the polypeptide was transformed into a very viscous homogeneous liquid. The results are discussed further in the study of the secondary structure.

Table 1. Molecular characteristics of the synthesized polypeptides

Polypeptide	M_n central P(*Boc*-L-Lys) x 10^{-3} (g/mol)[a]	N PLys central block[b]	M_n triblock PHIS/PBLG/PLys/total x 10^{-3} (g/mol)[a]	N PHIS/PBLG[c]	M_n Protected Pentablock x 10^{-3} (g/mol)[a]	N total external PLys/Mn x 10^{-3} protected[d]	Mn Deprotected Pentablock x 10^{-3} (g/mol)[e]	I[a]
PHIS100	46.3	203	45.4/0/46.3/91.7	120/0	119.5	122/27.8	58.0	1.1
PHIS30	45.8	201	13.2/18.6/45.8/77.6	35/85	105.2	121/27.6	64.6	1.12
PHIS50	45.1	198	23.1/13.1/45.1/81.3	61/60	108.7	120/27.4	62.2	1.09
PHIS70	46.0	202	31.4/7.7/46.0/85.1	83/35	113.4	124/28.3	60.8	1.16

[a)] Obtained by SEC-TALLS in DMF with 0.1 N LiBr at 60 ^{o}C; [b)] Calculated from the molecular weight obtained by SEC-TALLS and the molecular weight of the protected monomeric unit of Boc-Lysine; [c)] Calculated from the molecular weights obtained by SEC-TALLS of the middle poly(Boc-L-lysine) block and the total molecular weight of the (PHIS-*co*-PBLG)-*b*-PLys-*b*-(PHIS-*co*-PBLG) triblock terpolypeptide; [d)] Calculated from the molecular weights obtained by SEC-TALLS of the middle poly(Boc-L-lysine) block, the total molecular weight of the (PHIS-*co*-PBLG)-*b*-PLys-*b*-(PHIS-*co*-PBLG) triblock terpolypeptide precursor and the total molecular weight of the pentablock; [e)] Calculated from the molecular weights obtained by SEC-TALLS of the protected pentablocks after cleavage of the Boc- and Trityl- protective groups.

C. Investigation of the 3D Structure of the Hydrogels through Circular Dichroism and Scanning Electron Microscopy (SEM).

SEM pictures were obtained for the polypeptidic hydrogel formed by the terpolypeptide PHIS50 at pH=7.4 and 6.6. For pH=7.4, a well-ordered 3D structure of interconnected nanofibers and thin nanosheets which holds the mixture in the hydrogel form is observed. On the contrary, the structure at lower value of pH=6.6 is akin to collapsed thick sheets with interconnecting thick fibers and larger voids, resembling a liquid-like structure (**Figure 1**).

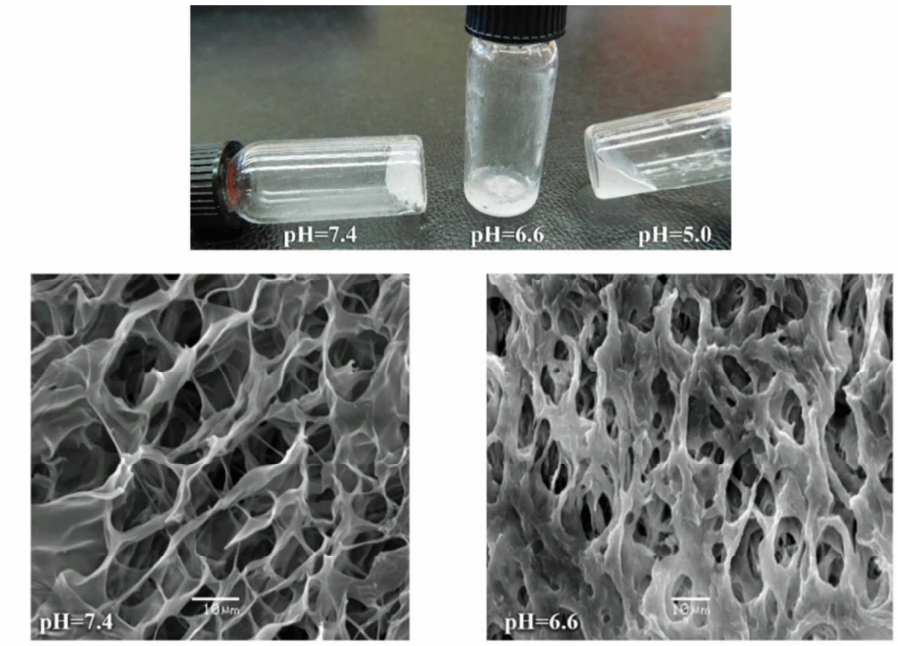

Figure 1. Top: Appearance of the hydrogel PHIS50 at different pH values as indicated. Bottom: Respective SEM images at pH=7.4 (left) and pH=6.6 (right).

Circular dichroism measurements were performed at concentrations below those used for the formation of hydrogels, in order to obtain liquid samples for placement in the cell, as well as to fall in a measurable concentration range. To date, only a few publications discuss the

synthesis of well-defined PHIS-containing polypeptides, hence the secondary structure of PHIS homopolypeptide at pH higher than its pKa value is not completely clear.[35] In previous publications, it was mentioned that at pH ≥7.4 PHIS forms *β*-sheets.[35-36] In our previous study[21] we found that PHIS exhibits a strong positive peak at 205 nm, a strong negative peak at 189nm, while there is also a weak negative peak at 225 nm. This secondary structure is attributed to a *β*-turn conformation.[37] This conformation has many different types, i.e. I, II and VI, depending on the values of dihedral angles of the amino acids. We found that the *β*-turn type I with φ_{+1}= -30^{o} and Ψ_{+1}= -60 is the most probable conformation. In these dihedral angle values, the imidazole groups take such a conformation to form intramolecular hydrogen bonds between the proton attached on the nitrogen of the imidazole ring of the monomeric unit N and the nitrogen of the imidazole monomeric unit N+3 (**Fig. 2a**, black arrows). In addition, typical hydrogen bonds between the hydrogen of the N monomer *α* carbon and of the N+3 monomer carbonyl group (**Fig. 2a**, yellow arrow) are also formed, as can be seen in **Figure 2a**. This renders PHIS at high pH values a model compound to study the *β*-turn conformation in a polypeptide exhibiting long-range conformational homogeneity, which is rather rare in nature but usually present in very short peptide sequences.

The CD spectra of the synthesized polypeptides are shown in **Figure 2b**. The dominant peak exhibits a strong negative signal at 197nm, corresponding to a random coil, which is attributed to the poly(L-lysine) conformation at neutral or low pH and partial protonation of the PHIS segment (**Figure 2b**). It is evident that the maximum of this peak shifts to higher wavelengths as the PBLG fraction increases. PBLG forms *α*-helices, and since these monomeric units do not respond to pH variation, it is expected that they maintain this conformation and exhibit the typical *α*-helix negative peaks at 222 and 208 nm, particularly for polypeptides with increased *γ*-benzyl-L-glutamate (BLG) composition.

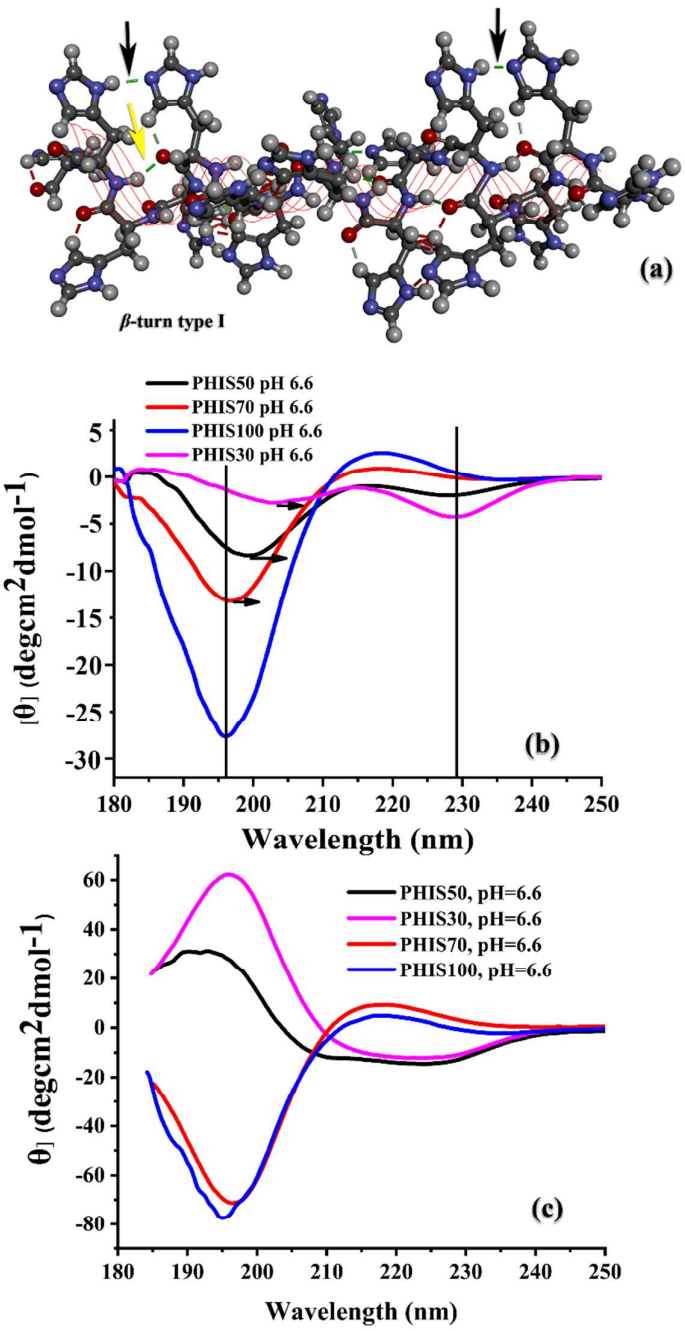

Figure 2. (a) Illustration of the secondary structure of PHIS homopolypeptide of *β*-turn type I. **(b)** Circular Dichroism spectra for the synthesized polypeptides at pH=6.6 **(c)** The CD spectra of the PBLG component of the terpolypeptides, obtained after the subtraction of the PLys and PHIS (in case of PHIS50 and PHIS30) component.

The two polypeptides (PHIS50 and PHIS30) that form a rather strong hydrogel exhibit a negative peak at 225-230cm^{-1}, which becomes stronger when PBLG fraction is increased. It is not clear from this spectra if this peak is due to the formation of a β-turn or is the result of the two secondary structures - the random poly(L-lysine) coil and the PBLG α-helix. For this reason, from the hydrogel spectrum we subtracted that of a solution of pure PLys (**SI Fig. S21**) having a concentration equal to that of PLys at the hydrogel, and the result is provided in **Figure 2c**. It can be seen that in the case of PHIS100 as well as PHIS70, PHIS shows the typical random coil conformation as expected for the PLys and PHIS conformation (negative peak at 195 nm and a positive peak at 222 nm, red and blue spectra) at this pH, while in the case of PHIS50 and PHIS30, the PBLG shows a typical α-helix conformation (positive peak at 190 nm and two negative peaks at 205 ans 225 nm, black and magenda). At pH=5.0, the hydrogel spectrum is not altered significantly, since almost all PHIS at pH=6.6 had already been transformed to random coil conformation (**SI Fig. S22, S23, S24**).

The two polypeptides that do not form strong hydrogels, i.e. PHIS100 and PHIS70 exhibit the typical peaks of the random coil conformation at pH=6.6 (Fig. 2c). This is the expected conformation for the PLys and PHIS at this pH. Concerning PHIS70, the random distribution of the BLG (30% molar ratio) along the PHIS monomeric units prohibits formation of α-helices or β-turn and thus the polypeptide does not form hydrogels. At the polypeptides PHIS50 and PHIS30, the increased BLG content gives these monomeric units the ability to form α-helices. Since the strong hydrogels are formed only at the terpolypeptides exhibiting PBLG with the *a*-helix conformation, it is evident that the presence of this secondary structure is critical for hydrogel formation.

D. Rheology.

In order for the hydrogel to be used as an effective delivery system, it is important to tailor the rheological properties of the hydrogel resulted from the synthesized polypeptide at the molecular level. Our aim was to combine different properties into a single material as follows: (a) pH-responsiveness within physiological pH values, i.e., weaker gel at the cancer tissue pH, while keeping its macroscopic cohesiveness and not becoming liquid, in which case the drug would need to be delivered in a burst-type way and not through a sustained slow-release procedure as is needed. (b) To exhibit shear thinning properties in order to become liquid-like at the shear rate range of a syringe operation in order to be injectable. (c) Very quick response times in order to self-heal quickly and to be reconstructed immediately when injected in the body (animal or human). (d) Sufficiently stable over time so that by applying the shear rate within the syringe to become a (reasonably homogeneous) liquid mixture and not collapse. (e) While applying shear by pushing the plunger, the viscosity of the resulting solution within the syringe should be sufficiently low to be easily extruded through a very thin 21G needle.

Dynamic Frequency Sweep (DFS) measurements of the PHIS100, PHIS50 and PHIS30 hydrogels at polypeptide concentration 3,33 % wt (or polypeptide/water ratio=1/30 w/w,) indicate that the strength (i.e., the effective pleteau storage modulus as extracted from the data, typically an average value of the nearly frequency-independent G' or its value at 1 rad/s) of PHIS100 hydrogel was weak, amounting to 200 Pa (**Fig. 3a**), therefore only the hydrogels formed by the polypeptide PHIS50 and PHIS30 were further studied (with plateau G' values of 2 and 7 kPa, respectively). The pH responsiveness of the PHIS30 hydrogel at physiological pH values between the cancer (pH=6.6) and healthy tissue (pH=7.4) as well as late endosomal pH (pH=6.0) was rather negligible, as seen in the strain sweeps of **Figure 3b,** which indicate same moduli values and the same solid-to-liquid transition with increasing strain, i.e. yielding. In this pH range the low-strain linear G' value ranged from 6 to 8 kPa. The respective

variation of the moduli crossover marking the yielding transition (at the measured frequency), beyond which the sample exhibits liquid-like response, is 2-5% in strain amplitude whereas the yield stress (determined by the product of crossover modulus and yield strain) is practically unchanged within experimental error. Beyond yielding in the nonlinear regime, the apparent moduli exhibit similar variance with pH with their low-strain analogues. See also **SI Fig. S15**.

In contrast to PHIS30, PHIS50 exhibited a pronounced pH dependence within the physiological pH range and particularly between the pH values of cancer and healthy tissues. Dynamic Sweep Frequency sweeps of PHIS50 at various pH ranges (**Fig. 3c**) showed that the polypeptide is rather strong (judged by its plateau G' of about 2kPa) and stable (repeated measurements were reproducible; they are not shown here), therefore we focused on this polypeptide. Initially, we examined the strength and the linear regime of the PHIS50 hydrogel at various concentrations without the drug at pH=7.4 and 37^{o}C, in order to find the appropriate concentration that would fulfill all requirements.

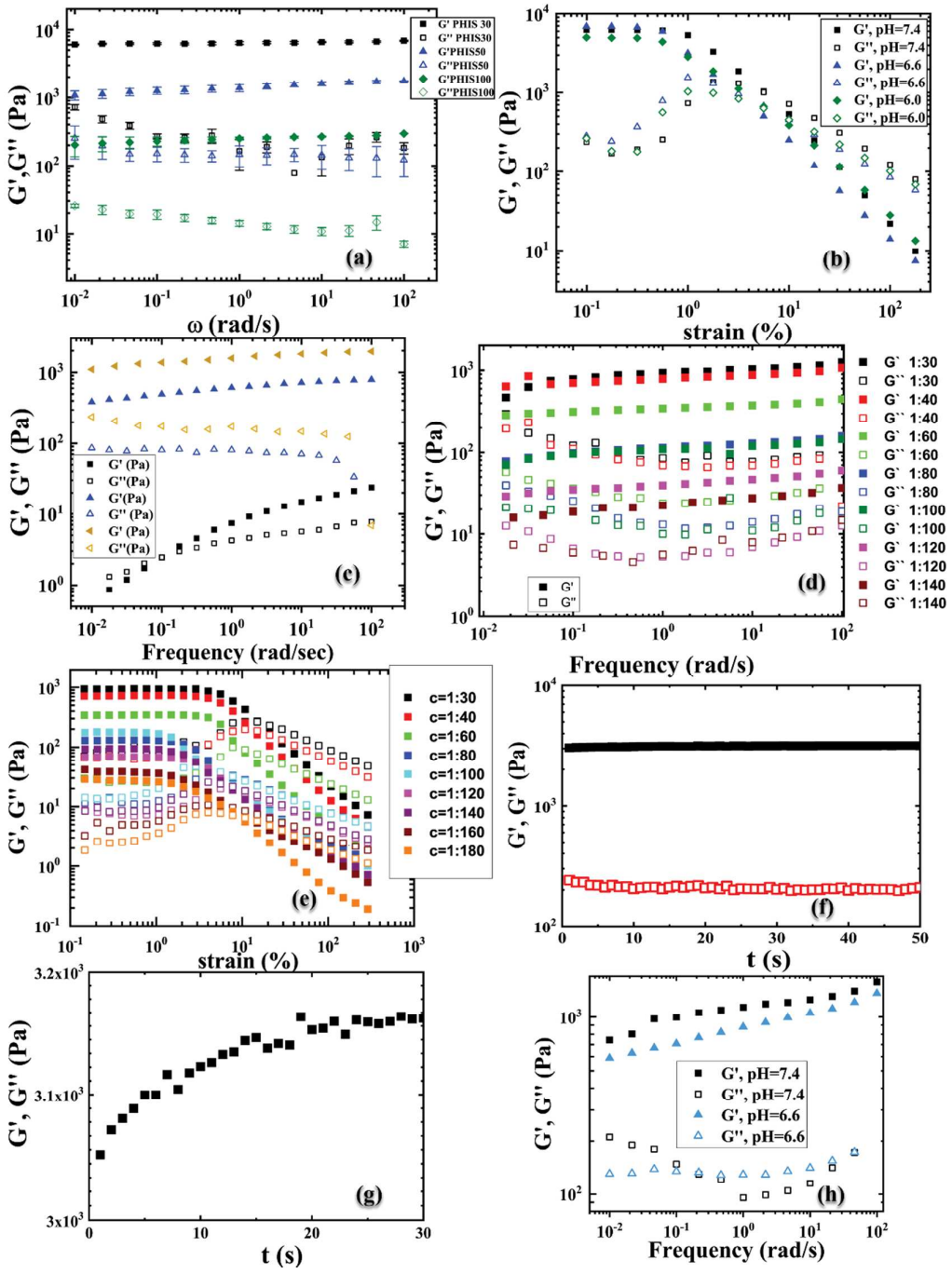

Figure 3. (a) Frequency-dependent storage G' and loss moduli G'' of the different hydrogels PHIS30, PHIS50, PHIS100 (all the polypeptide concentration 3.33% wt, pH=7.4). **(b)** Dynamic strain sweeps of the strongest hydrogel (PHIS30) at different values of pH (see text), indicating a weak variation of moduli and of the onset of yielding (solid to liquid transition). **(c)** Dynamic frequency sweeps of PHIS50 at different values of pH at concentration 1:30 w/w,

see text. All measurements were performed at 37 ^{o}C. **(d)** Viscoelastic moduli G' and G'' at different hydrogel concentrations with PHIS 50, pH 7.4 at 37 ^{o}C, as functions of angular frequency and **(e)** strain amplitude. **(f)** Self-healing test for hydrogel PHIS50 at pH 7.4, concentration 3.33% (w/w) and temperature 37 ^{o}C. **(g):** Self-healing test for hydrogel PHIS50 at pH 7.4, concentration 3.33% (w/w) and temperature 37 ^{o}C. G' as a function of time for very low time values. See text for details. **(h)** Frequency-dependent moduli G' (filled symbols) and G'' (empty symbols) at different pH for the gemcitabine-loaded hydrogel PHIS50 at concentration 1:30 at 37 ^{o}C. Black squares and blue triangles represent pH 7.4 and 6.6, respectively.

Rheometric measurements at various polypeptide/water concentrations (w/w) indicated that by lowering the polypeptide concentration, the storage modulus G', loss modulus G'' as well as the value of strain (**Fig. 3d and 3e**) diminished. For example, comparing the plateau G' values of concentrations 1/30, 1/60 and 1/140, we observe a decrease from 1000 to 400 to 30, respectively (Fig.3d). Likewise, from Fig.3e we observe a variation of linear G' value and yield strain from 1000 to 400 and from 20% to 10% as the concentration decreases from 1/30 to 1/60, respectively. In addition, at a concentration 1/30 the polypeptide transformed from a relatively strong hydrogel (with plateau G' of 2 kPa) at healthy tissue pH=7.4 to a weak hydrogel (with plateau G' of 800 Pa) at pH=6.6, to a viscoelastic liquid, at lower pH=6.0. The pH of cancer tissue can be vary from 6.0 to 6.8, depending on the conditions. (Fig. 3c). Remarkably, while the pH dependence was very strong, the temperature did not influence the strength of the polypeptide at any pH (see Fig.S15).

Through the rheological measurements, it was found that the hydrogel of the polypeptide PHIS50 was becoming liquid under the shear rate of 0.35 s^{-1}, which is the value obtained

from the crossover DSS to strain amplitude multiplied with the frequency, which is 1 rad/s. This is the minimum shear rate that should be applied to start making liquid the hydrogel. Applying a higher frequency, the viscosity of the liquid becomes lower. It was found that we needed less than 3 seconds to inject 0.085 ml of the hydrogel into the body of the mice. Thus, the syringe operated with a flow rate of 0.028 ml/s. Since the inner diameter of the 21G needle of the syringe was 0.08 cm, and assuming a Poiseuille flow, the applied shear rate by pushing the plunger was the flow rate of the liquid hydrogel divided by the cross section of the surface of the needle multiplied by the radius of the needle. Therefore, the shear rate equals (0.028 ml/s)/(3.14 x R^3), where R=0.04 cm. This amounts to an apparent shear rate of 140 s^{-1}, significantly higher than 0.35 s^{-1} required. It was found that by using the 1 ml syringe at a polypeptide/water=1/30 (w/w) concentration and a 21G needle, the polypeptide viscosity of PHIS50 enabled easy and quick extrusion through this needle, (the conditions of interest for in-vivo experiments) due to the high shear rate applied, and this concentration was employed for all the subsequent experiments. All these properties fulfilled the requirements (a) and (d) above.

In order to examine whether requirements (b), (c) and (e) could be fulfilled, the self-healing potential of the hydrogel was exploited. To this end, a shear rate of 0.35 s^{-1} was applied to the hydrogel, transforming it into a liquid. The shear rate was then stopped, and the time required to return to exactly the same G' value was recorded (**Fig. 3f**). Under healthy conditions, i.e. pH=7.4 and 37 ^{o}C, it was found that the time required for the hydrogel to return to 97% of its initial G' value was as low as 1 second, whereas an additional 14-16 seconds were needed in order to reach the exact initial value, yielding 100% recovery (**Figure 3g**). We repeated this experiment by synthesizing many different batches of pentablocks, trying to maintain the molecular characteristics, and the time was always on the order of a few seconds. This remarkably fast recovery time was required to ensure complete control of the implantation

within the body of the mouse. It was also found that concentration (polypeptide/water ratio w/w) and pH influenced the time required for the hydrogel to self-heal. By lowering the pH to 6.6, the self-healing time required to recover to the 97% of the initial value was 8 seconds, and about 60 more seconds were needed to recover completely (**SI Fig. S16**, **inset**). By lowering the concentration of the solution, the time increased significantly (**SI Fig. S18**). It was also found that the self-healing recovery time was not influenced by the presence of gemcitabine when we measured the hydrogel loaded with the drug (hydrogem) (results not shown).

We note that the pentablock macromolecular architecture was very crucial for quick self-healing, as the corresponding triblock terpolypeptide poly(L-lysine)-*b*-poly(L-histidine-*co*-*γ*-benzyl-L-glutamate)-*b*-poly(L-lysine) without the outer poly(L-lysine) blocks resulted in significantly larger self-healing times than the pentablock terpolypeptide. In addition, lower strength was obtained for the same concentration, pH and temperature (**SI Fig. S17**).

To interpret the above results, we propose that the presence of the outer poly(L-lysine) chains forces the hydrophobic chains to become well-oriented. In addition, the presence of two hydrophobic blocks in the same molecule induces strong organization of the chains either as loops or in parallel orientation, resulting in a well-defined 3D interconnected nanostructure surrounded by an aqueous environment (**SI Fig. S28**). This picture is supported from evidence in the literature. Bekard et al.[38] and Ashton et al.[39] investigated a protein under shear rate by a combination of rheology and Circular Dichroism and found that the shear rate induces the unfolding of *α*-helices, therefore the self-organization of the two *α*-helices is lost, however not all of them are transformed into the random coil conformation. The presence of two *α*-helices per polypeptidic chain affords the molecules a "memory" through the undisordered structures, and the molecules rapidly return to their initial structure upon shear cessation, leading immediately to reconstruction of the *α*-helices. (**SI Fig. S28)**.

From the above it follows that the "empty" hydrogel presented excellent *in-vitro* properties, however we had to assess the effect of gemcitabine on these properties. Gemcitabine is a hydrophilic drug that should remain in the aqueous phase, therefore its addition to the hydrogel was not expected to significantly alter the hydrogel rheological behavior. The most important parameter to control was the drug release rate. In order to directly relate the hydrogel rheological properties to the hydrogem stability and duration the mouse body, we subcutaneously injected healthy mice with hydrogels of the same polypeptide at different concentrations and therefore different plateau modulus G'. The results are provided in **Table 2**. In all cases, the variance between measurements was less than 15%.

Table 2. Influence of the storage modulus G' on the time needed for the hydrogel to transform into a liquid in the body of a healthy mouse.

Concentration (polypeptide/water w/w)	Storage Modulus G' at 1 rad/sec (Pa)	Duration of the Polypeptide (days)
1/30	1010.2	50
1/40	830.3	8
1/60	346.0	2
1/80	155.8	-

For a concentration of 1/30, the duration of the hydrogel within the body was 50 days. Therefore, for the hydrogem, the 1/30 polypeptide/water concentration was used, while the amount of gemcitabine in this gel was equal to that of the polypeptide.

We performed rheological measurements of the hydrogel loaded with gemcitabine at a polypeptide concentration 1/30 (polypeptide/water (w/w)) and drug concentration 1/30 (drug/water (w/w)). It was found that the presence of the drug resulted in a slight

strengthening of the hydrogel at pH=7.4 and 37^{o}C (**Fig. 3h**). There is also a slightly stronger decrease of moduli with decreasing frequency at both pH=7.4 and 6.6 in hydrogems compared to hydrogels without drug (see Fig.3a,d). Note that at pH=6.6 and temperature 37^{o}C, the decrease of the storage modulus (at 1 rad/s) of hydrogem compared to the one at healthy conditions is not as high as in the case of the hydrogel without the drug at the same temperature and pH (Fig.S19). This indicates a strong interaction of the drug with the hydrophobic part of the hydrogel, which directs the responsiveness. Gemcitabine is considered to be hydrophilic. However, we found that it was not soluble at the concentration 33 mg/mL required for the formation of the hydrogels, and heating at 40 degrees was required in order to keep it soluble. The presence of an aromatic ring in the molecule of gemcitabine is expected to interact with the aromatic ring of PBLG units, and this has affected the rheological properties of the hydrogem. This interaction between the drug and the polypeptide is expected to keep the drug encapsulated within the hydrogel, and thus, present limited release under healthy conditions. This is a requirement for the targeted delivery of the drug along with the degradation of the hydrogel at the vicinity of the cancer tissue, mainly due to the responsiveness on pH. The drug has to be released together with the polypeptide when the hydrogel becomes liquid under the cancer tissue conditions, probably encapsulated within an aggregate formed by the polypeptide. Since PHIS exhibits a strong "proton sponge mechanism",[23] it is expected to enable the rupture of the endosome when the aggregate is inserted into the cancer cell and enhance drug efficacy compared to delivery of the drug alone.

E. Enzymatic Degradation.

Recently, the utilization of enzymes as a stimuli has received a great deal of attention for drug delivery by vesicles.[40] Advances in the field of synthetic biomaterials have added the enzymatic degradation of the polypeptide-based hydrogels as a further advantage of those

systems, offering a new stimulus for their drug release applications and establishing biodegradation as an important property.[41-43] However, the evaluation of the sensitivity of these hydrogels to proteases has not yet been reported. Cancer cells often secrete proteolytic enzymes that can act as a stimulus for polypeptidic materials to release their cargo. Our hydrogels, due to their polypeptide nature, could take advantage of this stimulus in order to release their drug cargo.

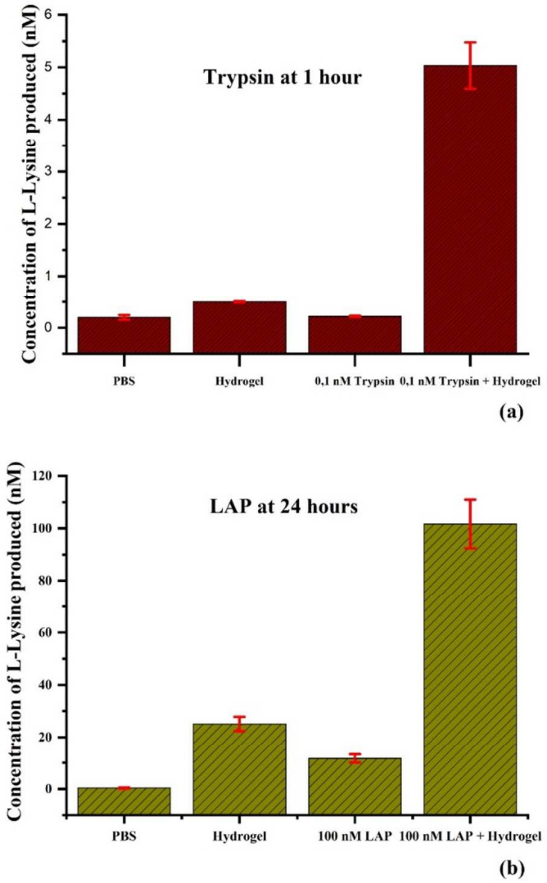

Figure 4. Biodegradation test of hydrogel PHIS50 by means of **(a)** Trypsin during 1 hour and **(b)** LAP during 24 hours of incubation at 37 ^{o}C. (see text for details).

Biodegradation is probably distinct from this stimulus as a biological process and may be mediated by the normal proteolytic activity of the extra-cellular matrix. Even if the cancer

cells are completely eliminated, the implanted hydrogel will be slowly degraded and will not need to be removed from the body, as in the case of other synthetic non-biodegradable polypeptides. Various enzymes can potentially participate in these biochemical processes. The hydrogel PHIS50 was tested against LAP (leucine aminopeptidase). LAP is an exopeptidase that catalyzes the hydrolysis of amino acid residues from the amino terminus of polypeptide chains and trypsin, an endopeptidase, which randomly cleaves the amide bond of lysine residues from its C-terminal side. Thus, free amino groups are produced during the degradation by each enzyme. A sample during the enzymatic reaction was removed at specific times and reacted with fluorescamine.[44] The product of this reaction is fluorescent and can be used to calculate the rate of enzymatic degradation of the hydrogel (**Fig. 4a, 4b**). For highest accuracy, the instrument was calibrated by the fluorescence induced by reaction of L-lysine with fluorescamine (SI, S25, S26). The hydrogel was found to be sensitive to degradation by both enzymes tested, although much more so for trypsin, possibly due to the reduced accessibility of the amino terminus of the polypeptide. The Specific Activity of LAP for PHIS50 was found to be $5.6 \times 10^{-6} \pm 1.7 \times 10^{-7}$ s^{-1} mg $hydrogel^{-1}$, while the value for Trypsine for the same hydrogel was $0.153 \pm 3.1 \times 10^{-5}$ s^{-1} mg $hydrogel^{-1}$. By increasing the degradation of the hydrogel, it was turning liquid insteat of soft solid. We have to mention that the concentrations of the enzymes used in this study was much higher to the one in the organism, and the degradation rate observed is not comparable to the one under *in vivo* conditions, which are expeced to be more slow.

F. Acute Toxicity in Mice.

The results of the *in-vivo* toxicity analysis suggested that the most appropriate hydrogel form to load the drug was that consisting of PBLG at a concentration of 1/30. The polypeptides containing PLEU at 1/30 were found to be toxic when administered

intraperitoneally (ip) since the recipient mouse died two days later. Additionally, the mice that received the 400 and 200mg/kg dose of these polypeptides suffered from severe skin irritation at the site of the injection (**SI Fig. S27**). Furthermore, the corresponding PLEU-containing PHIS50 hydrogel quickly disappeared after the subcutaneous administration, suggesting that this form was unstable. This might be due to the presence of enzymes that degrade the LEU amide bonds more quickly than those of BLG, since they presented similar rheological behavior. Unlike PLEU, the PBLG hydrogel demonstrated more favorable properties. It was non-toxic at all doses, with slight skin irritation being the most obvious side effect only at the higher dose, while remaining profoundly visible at the site of injection for substantially more time (up to two weeks post administration). These results suggested that PBLG was the most stable, nontoxic and thus most suitable hydrogel form for gemcitabine loading (**Fig. 5a, 5b, 5c**).

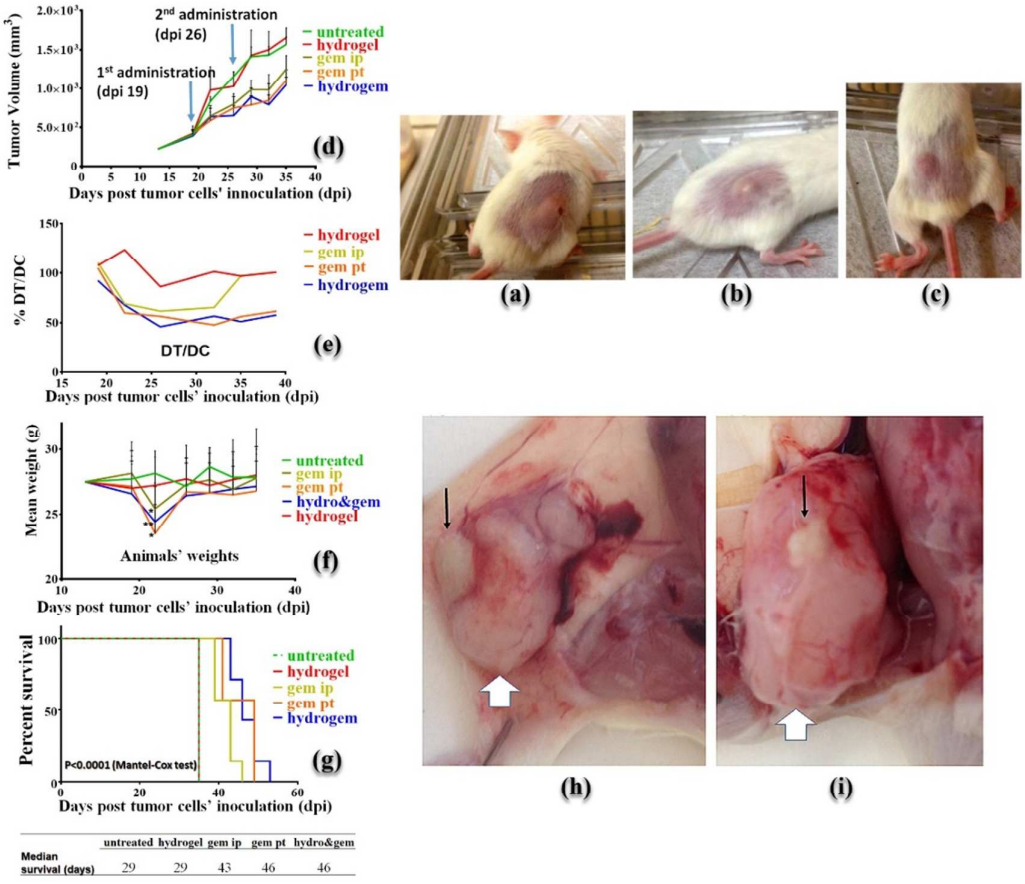

	untreated	hydrogel	gem ip	gem pt	hydro&gem
Median survival (days)	29	29	43	46	46

Figure 5. Toxicity tests of empty pentablock terpolypeptide PHIS50, **(a)**: 400 mg/Kg, **(b)**: 200 mg/kg, **(c):** 100 mg/Kg. Hydrogem efficacy in AsPC-1 human pancreatic xenografts developed in NOD.CB17Prkdc^{scid}/J mice. **(d)** Tumor growth curve of AsPC-1 xenografts. Each point shows the mean ± SD. All time points beyond d.p.i 20 were statistically significant at $p<0.0001$ vs untreated and hydrogel-treated groups (Two-way ANOVA, Dunnett post hoc test). Arrows show the time points of the administrations **(e)** % DT/DC ratios for all groups. **(f)** Animal mean weights. Each point shows the mean ± SD. Each point shows the mean ± SD. *, $p<0.05$ vs untreated; **, $p<0,01$ vs untreated **(g)** Kaplan-Meier survival curve for AsPC1 xenografts. Table of Figure **(g)** shows the median survival in days for the five groups.

Gem ip; mice receiving intraperitoneal and gem pt; mice receiving peritumoral injections of 100mg/kg gemcitabine at days 19 and 26. Hydrogem mice receiving peritumoral injections of gemcitabine-loaded hydrogel at 100mg/kg at day 19 post inoculation of the tumor cells. Untreated; mice receiving no treatment. Hydrogel; mice receiving empty hydrogels.

Photos showing the hydrogem (thin black arrows) as it appeared one week **(h)** and four weeks **(i)** post its peritumoral administration in AsPC-1 xenografted tumors (thick white arrows).

G. Efficacy study in xenografts.

The efficacy of the gemcitabine-loaded hydrogel was tested on human to mouse xenografts. Our goal was to have the highest possible deceleration of the tumor growth with minimum use of drug and minimum number of doses, without the presence of the drug to change the properties of the hydrogel. Therefore, we had to identify if the hydrogel would present a sustained release of a drug for about a month compared to the delivery of pure gemcitabine, with less drug and less injections. For that purpose, we delivered 40% of the encapsulated drug through the injected hydrogem (hydrogel+gemcitabine) in one dose, and compared to the

delivery of 100% of pure gemcitabine ip or pt delivered in two doses. As described in the experimental section, one group (untreated) received nothing and served as the control group. As positive controls, a second and third group received gemcitabine either ip or peritumorally (pt) (gem ip and gem pt groups), a fourth group received unloaded hydrogel and served as a negative control (hydrogel group) while the fifth group received the hydrogem pt. The pure gemcitabine groups received two injections of the chemotherapeutic drug at a week interval and a dose of 100mg/kg/injection/mouse. i.e. 200 mg of gemcitabine total. The hydrogem group received only a single injection with 83µl of the hydrogem corresponding to a slightly lower dose (80 mg/kg) of gemcitabine, while the hydrogel group received 83µl of unloaded hydrogel. Therefore, we delivered 80 mg/Kg/mouse of drug through hydrogem, and 200 mg/Kg/mouse of pure drug total, i.e. we delivered only 40% of the drug through hydrogem, as compared to the amount of pure drug delivered in two doses.

The subsequent efficacy study suggested that the combination of hydrogel with gemcitabine was superior to the administration of the drug alone as compared to both routes of administration (ip or pt) under the experimental conditions tested. Indeed, gemcitabine delivery resulted in the same level of tumor growth delay (**Fig. 5d and 5e**) when administered pt in the hydrogel form at a total dose equivalent to only 40% of the free drug administered pt. It is noteworthy that gemcitabine administered pt was found to be slightly superior to gemcitabine administered ip. Both the gemcitabine-loaded hydrogel and gemcitabine administered pt resulted in improved DT/DC ratios compared to the ip administered drug (**Fig. 5e**), very close to 40%. Additionally, as judged from the DT/DC ratios, this delay in tumor growth was sustained until the end of the experiment. No significant toxicity was observed as weight loss in the mice. Some weight loss observed in all groups that received the pure drug was only transient and the mice soon recovered the weight lost (**Fig. 5f**).

The Kaplan-Meier survival curve showed that hydrogem was superior to that of free gemcitabine as it increased the life span of the recipient mice more than the free drug did (Fig. 5g), with only 40% of the drug as and in one dose, as compared with the amount used when administered the drug alone.

Finally, autopsies preformed on euthanized mice revealed that hydrogem remained preferably adhered to the cancer rather than healthy tissue thereby increasing the selective delivery of the drug (**Fig. 5h and 5i**), while the reduction in the volume observed may be indicative of the pH-responsiveness as well as the biodegradation of the hydrogel.

CONCLUSIONS

Over the last 40 years, impressive advancements towards the discovery of novel drugs as well as responsive multifunctional drug delivery systems (DDS) have been reported. As a consequence, out of more than 200 different cancers, some highly lethal cancers are now chronic diseases. Unfortunately, only limited progress has been made for some specific forms of cancer, such PC. For this complex disease, very sophisticated carriers should be designed to bypass biological barriers with minimum cargo loss and effective and selective delivery to the desired pathological site, as demonstrated by the material described in this work.

For many years, our group has been synthesizing polypeptidic materials with complex macromolecular architectures, in order to elucidate the structure-properties relationship. Using this experience, we developed an amphiphilic pentablock terpolypeptide by optimizing the macromolecular architecture, composition as well as the 3D structure of the hydrophobic blocks. The final pentablock terpolypeptide exhibits a unique combination of properties in the same molecule which has not been achieved so far. Simply, by mixing the polypeptide and gemcitabine dissolved in water results in the facile formation of an injectable and quickly self-healing hydrogel which forms *in-situ* and can be injected in the least invasive way close to

cancer tissue. These properties rely on the secondary structure of the hydrophobic part of the amphiphilic terpolypeptide. After implantation, the hydrogel becomes liquid only close to the cancer tissue, mainly due to the lower pH of the pathological site, thus releasing the drug only in the vicinity of cancer tissue. This obliges the directional release of the drug towards the cancer rather than healthy tissue, as shown by *in-vivo* experiments**.** It was found that the delivery of only 40% of gemcitabine in one dose directed by the hydrogel, could slow down the development of the cancer tissue to the same extend with the delivery of 100% of pure gemcitabine in two doses, the typical chemotherapy used so far in clinics. Therefore, we achieved the same or slightly better deceleration of tumor growth with less drug and fewer number of doses, due to the guided delivery through the hydrogem. The hydrogel also responds to enzymes, rendering it biodegradable thus not requiring removal through resection following drug delivery. The synthesized material is modular since its properties can be modified by its molecular characteristics to deliver other drugs, rendering it very useful for a variety of biological applications, such as bone regeneration, catheters for treatment of coronary artery disease etc. We intend to improve the hydrogel effectiveness by incorporating more stimuli, such as temperature and redox, in order to increase selectivity for targeting cancer cells.

We believe that the synergy of material and pharmaceutical scientists, biologists and clinical oncologists is imperative to produce efficient DDS that possess advanced properties and required functionalities to fight this pancreatic cancer. The present work is a testimony of this important function.

ASSOCIATED CONTENT

Supporting Information. The full details concerning the synthesis and characterization of the monomers and the polypeptidic materials, as well as the methods used, are given in this

section. In addition, the synthesis, characterization and properties of the hydrogels resulted from the pentablocks having poly(L-leucine), instead of poly(γ-benzyl-L-blutamate) is given. Finally, the *in-vivo* tests of the pentablocks containing poly(L-leucine) instead of poly(γ-benzyl-L-blutamate) is given. "This material is available free of charge via the Internet at http://pubs.acs.org."

AUTHOR INFORMATION

Corresponding Author

***Hermis Iatrou, E-mail:** iatrou@chem.uoa.gr, **Address:** University of Athens, Chemistry Department, Panepistimiopolis, Zografou, 15771, Athens, Greece.

Author Contributions

The manuscript was written through contributions of all authors. The project was conceived and directed by H.I. The synthesis of the terpolypeptides were performed by P.B., A. K and D.S under the guidance of H.I.. Rheology were conducted by J. M. under the guidance of D. V. Enzymatic degradation measurements were performed by A. S. and D. S. under the guidance of Efstratios Stratikos. *In-vivo* measurements were conducted by Evang. Sereti, C. T. under the guidance of K. D.

ACKNOWLEDGMENT

This research was co-financed by the European Union (European Social Fund – ESF) and Greek national funds through the Operational Program ''Education and Lifelong Learning'' of the National Strategic Reference Framework (NSRF) - Research Funding Program: Aristeia I acronym PANNANOMED code 1055 and Thalis acronym META-SSEMBLY code 379436.

ABBREVIATIONS

HIS-NCA, N^{im}-trityl protected L-histidine N-carboxy anhydride; BLG-NCA, γ-benzyl-L-glutamate N-carboxy anhydride; PLys, poly(L-lysine); PLEU, poly(L-leucine); PBLG, poly(γ-benzyl-L-glutamate).

REFERENCES

1. Siegel, R. L.; Miller, K. D.; Jemal, A., Cancer Statistics, 2017. *CA-A Cancer J. Clin.* **2017,** *67* (1), 7-30.

2. Olive, K. P.; Jacobetz, M. A.; Davidson, C. J.; Gopinathan, A.; McIntyre, D.; Honess, D.; Madhu, B.; Goldgraben, M. A.; Caldwell, M. E.; Allard, D.; Frese, K. K.; DeNicola, G.; Feig, C.; Combs, C.; Winter, S. P.; Ireland-Zecchini, H.; Reichelt, S.; Howat, W. J.; Chang, A.; Dhara, M.; Wang, L. F.; Ruckert, F.; Grutzmann, R.; Pilarsky, C.; Izeradjene, K.; Hingorani, S. R.; Huang, P.; Davies, S. E.; Plunkett, W.; Egorin, M.; Hruban, R. H.; Whitebread, N.; McGovern, K.; Adams, J.; Iacobuzio-Donahue, C.; Griffiths, J.; Tuveson, D. A., Inhibition of Hedgehog Signaling Enhances Delivery of Chemotherapy in a Mouse Model of Pancreatic Cancer. *Science* **2009,** *324* (5933), 1457-1461.

3. Zhong, H.; De Marzo, A. M.; Laughner, E.; Lim, M.; Hilton, D. A.; Zagzag, D.; Buechler, P.; Isaacs, W. B.; Semenza, G. L.; Simons, J. W., Overexpression of hypoxia-inducible factor 1 alpha in common human cancers and their metastases. *Cancer Res.* **1999,** *59* (22), 5830-5835.

4. De Monte, L.; Reni, M.; Tassi, E.; Clavenna, D.; Papa, I.; Recalde, H.; Braga, M.; Di Carlo, V.; Doglioni, C.; Protti, M. P., Intratumor T helper type 2 cell infiltrate correlates with cancer-associated fibroblast thymic stromal lymphopoietin production and reduced survival in pancreatic cancer. *J. Exp. Med.* **2011,** *208* (3), 469-478.

5. Wilhelm, S.; Tavares, A. J.; Dai, Q.; Ohta, S.; Audet, J.; Dvorak, H. F.; Chan, W. C. W., Analysis of nanoparticle delivery to tumours. *Nat. Rev. Materials* **2016,** *1* (5).

6. Altunbas, A.; Pochan, D. J., Peptide-Based and Polypeptide-Based Hydrogels for Drug Delivery and Tissue Engineering. In *Peptide-Based Materials*, Deming, T., Ed. 2012; Vol. 310, pp 135-167.

7. Loebel, C.; Rodell, C. B.; Chen, M. H.; Burdick, J. A., Shear-thinning and self-healing hydrogels as injectable therapeutics and for 3D-printing. *Nat. Protocols* **2017,** *12*, 1521.

8. Guvendiren, M.; Lu, H. D.; Burdick, J. A., Shear-thinning hydrogels for biomedical applications. *Soft Matter* **2012,** *8* (2), 260-272.

9. Oh, H. J.; Joo, M. K.; Sohn, Y. S.; Jeong, B., Secondary Structure Effect of Polypeptide on Reverse Thermal Gelation and Degradation of L/DL-Poly(alanine)-Poloxamer-L/DL-Poly(alanine) Copolymers. *Macromolecules* **2008,** *41* (21), 8204-8209.

10. Choi, Y. Y.; Joo, M. K.; Sohn, Y. S.; Jeong, B., Significance of secondary structure in nanostructure formation and thermosensitivity of polypeptide block copolymers. *Soft Matter* **2008,** *4* (12), 2383-2387.

11. Kim, J. Y.; Park, M. H.; Joo, M. K.; Lee, S. Y.; Jeong, B., End Groups Adjusting the Molecular Nano-Assembly Pattern and Thermal Gelation of Polypeptide Block Copolymer Aqueous Solution. *Macromolecules* **2009,** *42* (8), 3147-3151.

12. Kim, E. H.; Joo, M. K.; Bahk, K. H.; Park, M. H.; Chi, B.; Lee, Y. M.; Jeong, B., Reverse Thermal Gelation of PAF-PLX-PAF Block Copolymer Aqueous Solution. *Biomacromolecules* **2009,** *10* (9), 2476-2481.

13. Choi, Y. Y.; Jang, J. H.; Park, M. H.; Choi, B. G.; Chi, B.; Jeong, B., Block length affects secondary structure, nanoassembly and thermosensitivity of poly(ethylene glycol)-poly(L-alanine) block copolymers. *J. Mater. Chem.* **2010,** *20* (17), 3416-3421.

14. Huang, J.; Hastings, C. L.; Duffy, G. P.; Kelly, H. M.; Raeburn, J.; Adams, D. J.; Heise, A., Supramolecular Hydrogels with Reverse Thermal Gelation Properties from (Oligo)tyrosine Containing Block Copolymers. *Biomacromolecules* **2013,** *14* (1), 200-206.

15. Joo, M. K.; Ko, D. Y.; Jeong, S. J.; Park, M. H.; Shinde, U. P.; Jeong, B., Incorporation of D-alanine into poly(ethylene glycol) and L-poly(alanine-co-phenylalanine)

block copolymers affects their nanoassemblies and enzymatic degradation. *Soft Matter* **2013,** *9* (33), 8014-8022.

16. Chen, Y.; Pang, X. H.; Dong, C. M., Dual Stimuli-Responsive Supramolecular Polypeptide-Based Hydrogel and Reverse Micellar Hydrogel Mediated by Host-Guest Chemistry. *Adv. Funct. Mater.* **2010,** *20* (4), 579-586.

17. Jang, J. H.; Choi, Y. M.; Choi, Y. Y.; Joo, M. K.; Park, M. H.; Choi, B. G.; Kang, E. Y.; Jeong, B., pH/temperature sensitive chitosan-g-(PA-PEG) aqueous solutions as new thermogelling systems. *J. Mater. Chem.* **2011,** *21* (14), 5484-5491.

18. Gerweck, L. E.; Seetharaman, K., Cellular pH gradient in tumor versus normal tissue: Potential exploitation for the treatment of cancer. *Cancer Res.* **1996,** *56* (6), 1194-1198.

19. Webb, B. A.; Chimenti, M.; Jacobson, M. P.; Barber, D. L., Dysregulated pH: a perfect storm for cancer progression. *Nat. Rev. Cancer* **2011,** *11* (9), 671-677.

20. Gallagher, F. A.; Kettunen, M. I.; Day, S. E.; Hu, D. E.; Ardenkjaer-Larsen, J. H.; in't Zandt, R.; Jensen, P. R.; Karlsson, M.; Golman, K.; Lerche, M. H.; Brindle, K. M., Magnetic resonance imaging of pH in vivo using hyperpolarized (13)C-labelled bicarbonate. *Nature* **2008,** *453* (7197), 940-U73.

21. Mavrogiorgis, D.; Bilalis, P.; Karatzas, A.; Skoulas, D.; Fotinogiannopoulou, G.; Iatrou, H., Controlled polymerization of histidine and synthesis of well-defined stimuli responsive polymers. Elucidation of the structure-aggregation relationship of this highly multifunctional material. *Polym. Chem.* **2014,** *5* (21), 6256-6278.

22. Pack, D. W.; Putnam, D.; Langer, R., Design of imidazole-containing endosomolytic biopolymers for gene delivery. *Biotechnol. Bioeng.* **2000,** *67* (2), 217-223.

23. Putnam, D.; Zelikin, A. N.; Izumrudov, V. A.; Langer, R., Polyhistidine-PEG:DNA nanocomposites for gene delivery. *Biomaterials* **2003,** *24* (24), 4425-4433.

24. Hamley, I. W.; Kirkham, S.; Dehsorkhi, A.; Castelletto, V.; Adamcik, J.; Mezzenga, R.; Ruokolainen, J.; Mazzuca, C.; Gatto, E.; Venanzi, M.; Placidi, E.; Bilalis, P.; Iatrou, H., Self-Assembly of a Model Peptide Incorporating a Hexa-Histidine Sequence Attached to an Oligo-Alanine Sequence, and Binding to Gold NTA/Nickel Nanoparticles. *Biomacromolecules* **2014,** *15* (9), 3412-3420.

25. Bilalis, P.; Tziveleka, L. A.; Varlas, S.; Iatrou, H., pH-Sensitive nanogates based on poly(L-histidine) for controlled drug release from mesoporous silica nanoparticles. *Polym. Chem.* **2016,** *7* (7), 1475-1485.

26. Bilalis, P.; Varlas, S.; Kiafa, A.; Velentzas, A.; Stravopodis, D.; Iatrou, H., Preparation of Hybrid Triple-Stimuli Responsive Nanogels Based on Poly(L-histidine). *J. Polym. Sci. Part A-Polym. Chem.* **2016,** *54* (9), 1278-1288.

27. Skoulas, D.; Stavroulaki, D.; Santorinaios, K.; Iatrou, H., Synthesis of Hybrid-Polypeptides m-PEO-b-poly(His-co-Gly) and m-PEO-b-poly(His-co-Ala) and Study of Their Structure and Aggregation. Influence of Hydrophobic Copolypeptides on the Properties of Poly(L-histidine). *Polymers* **2017,** *9* (11).

28. Hadjichristidis, N.; Iatrou, H.; Pispas, S.; Pitsikalis, M., Anionic polymerization: High vacuum techniques. *J. Polym. Sci. Part A-Polym. Chem.* **2000,** *38* (18), 3211-3234.

29. Hadjichristidis, N.; Iatrou, H.; Pitsikalis, M.; Sakellariou, G., Synthesis of Well-Defined Polypeptide-Based Materials via the Ring-Opening Polymerization of alpha-Amino Acid N-Carboxyanhydrides. *Chem. Rev.* **2009,** *109* (11), 5528-5578.

30. National Cancer Institute, N., NIH https://dtp.cancer.gov/organization/btb/acute_toxicity.htm.

31. Delyon, J.; Varna, M.; Feugeas, J. P.; Sadoux, A.; Yahiaoui, S.; Podgorniak, M. P.; Leclert, G.; Dorval, S. M.; Dumaz, N.; Janin, A.; Mourah, S.; Lebbe, C., Validation of a

preclinical model for assessment of drug efficacy in melanoma. *Oncotarget* **2016,** *7* (11), 13069-13081.

32. Li, Z. B.; Deming, T. J., Tunable hydrogel morphology via self-assembly of amphiphilic pentablock copolypeptides. *Soft Matter* **2010,** *6* (11), 2546-2551.

33. Schwyzer, R.; Rittel, W., Synthese von Peptid□Zwischenprodukten für den Aufbau eines corticotrop wirksamen Nonadecapeptids. I. Nϵ□t□Butyloxycarbonyl□L□lysin, Nϵ□(Nϵ□t□Butyloxycarbonyl□L□lysyl)□Nϵ□t□butyloxycarbonyl□L□lysin, Nϵ□t□Butyloxycarbonyl□L□lysyl□L□prolyl□L□valyl□glycin und Derivate. *Helv. Chim. Acta* **1961,** *44* (1), 159-169.

34. Bergmann, M.; Zervas, L., Über ein allgemeines Verfahren der Peptid□Synthese. *Ber. Dtsch. Chem. Ges. (A and B Series)* **1932,** *65* (7), 1192-1201.

35. Myer, Y. P.; Barnard, E. A., Structure-reactivity relations of imidazole in polypeptides: I. Structural transitions and a β-structure in poly-l-histidine solutions. *Arch. Biochem. Biophys.* **1971,** *143* (1), 116-122.

36. Peggion, E.; Cosani, A.; Terbojevich, M.; Scoffone, E., Solution Properties of Synthetic Polypeptides. Circular Dichroism Studies on Poly-L-histidine and on Random Copolymers of L-Histidine and L-Lysine in Aqueous Solution. *Macromolecules* **1971,** *4* (6), 725-731.

37. Brahms, S.; Brahms, J., Determination of protein secondary structure in solution by vacuum ultraviolet circular dichroism. *J. Mol. Biol.* **1980,** *138* (2), 149-178.

38. Bekard, I. B.; Barnham, K. J.; White, L. R.; Dunstan, D. E., α-Helix unfolding in simple shear flow. *Soft Matter* **2011,** *7* (1), 203-210.

39. Ashton, L.; Dusting, J.; Imomoh, E.; Balabani, S.; Blanch, E. W., Susceptibility of different proteins to flow-induced conformational changes monitored with Raman spectroscopy. *Biophys. J.* **2010,** *98* (4), 707-14.

40. Chandrawati, R., Enzyme-responsive polymer hydrogels for therapeutic delivery. *Exp. Biol. Med.* **2016,** *241* (9), 972-979.

41. Hayashi, T.; Kanai, H.; Yodoya, S.; Oka, M.; Hayashi, T., Biodegradation of random co-polypeptide hydrogels consisting of N-hydroxypropyl L-glutamine as one component. *Eur. Polym. J.* **2002,** *38* (1), 139-146.

42. Thornton, P. D.; Billah, S. M. R.; Cameron, N. R., Enzyme-Degradable Self-Assembled Hydrogels From Polyalanine-Modified Poly(ethylene glycol) Star Polymers. *Macromol. Rapid Commun.* **2013,** *34* (3), 257-262.

43. Jeong, Y.; Joo, M. K.; Bahk, K. H.; Choi, Y. Y.; Kim, H.-T.; Kim, W.-K.; Jeong Lee, H.; Sohn, Y. S.; Jeong, B., Enzymatically degradable temperature-sensitive polypeptide as a new in-situ gelling biomaterial. *J. Controlled Release* **2009,** *137* (1), 25-30.

44. Bantan-Polak, T.; Kassai, M.; Grant, K. B., A comparison of fluorescamine and naphthalene-2,3-dicarboxaldehyde fluorogenic reagents for microplate-based detection of amino acids. *Anal. Biochem.* **2001,** *297* (2), 128-136.

TABLE OF CONTENTS (TOC)

Self-Healing pH- and Enzyme Stimuli-Responsive Hydrogels for Targeted Delivery of Gemcitabine to Treat Pancreatic Cancer

Panayiotis Bilalis, Dimitrios Skoulas, Anastasios Karatzas, John Marakis, Athanasios Stamogiannos, Chrisida Tsimblouli, Evangelia Sereti, Efstratios Stratikos, Konstantinos Dimas, Dimitris Vlassopoulos and Hermis Iatrou

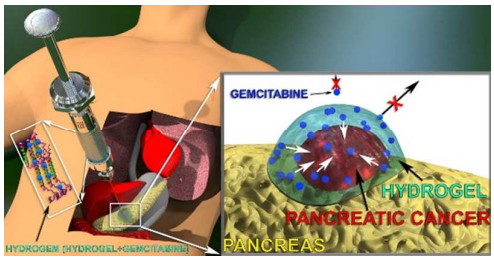

A hydrogel is developed that forms very easily after mixing an aqueous solution of gemcitabine with a novel polypeptide. It exhibits shear-thinning properties and can be implanted *in-situ* in the least invasive way. It has short self-healing time required to be reconstructed quickly to be deposited close to the cancer tissue. It responds and melts close to the lower extracellular pH values of the cancer thus delivering directionally gemcitabine towards the cancer tissue . The hydrogel is enzymatically biodegradable, and thus does not require resection after cargo delivery.